DALTON
FULL PAPER

Triruthenium–iridium clusters containing alkyne ligands: synthesis, structure, and catalytic implications of $[(\mu\text{-H})IrRu_3(CO)_{11}(\mu_3\text{-}\eta^2\text{-}PhC{\equiv}CPh)]$ and $[IrRu_3(CO)_{10}(\mu_4\text{-}\eta^2\text{-}PhC{\equiv}CPh)(\mu\text{-}\eta^2\text{-}PhC{=}CHPh)]$

Vincent Ferrand, Georg Süss-Fink,* Antonia Neels and Helen Stoeckli-Evans

Institut de Chimie, Université de Neuchâtel, CH-2000 Neuchâtel, Switzerland

Received 27th July 1998, Accepted 9th October 1998

The mixed-metal cluster $[HIrRu_3(CO)_{13}]$ **1** reacts with one equivalent of disubstituted alkynes RC≡CR to give $[HIrRu_3(CO)_{11}(\mu_3\text{-}\eta^2\text{-}RC{\equiv}CR)]$ (R = Ph **2**; R = Me **3**), with a second equivalent of the alkyne the clusters $[IrRu_3(CO)_{10}(\mu_4\text{-}\eta^2\text{-}RC{\equiv}CR)(\mu\text{-}\eta^2\text{-}RC{=}CHR)]$ (R = Ph **4**; R = Me **5**) are obtained. The single-crystal X-ray structure analyses of **2** and **3** show these clusters to have a tetrahedral Ru_3Ir framework containing the alkyne ligand coordinated in a parallel fashion over the Ru_3 face of the metal skeleton. In contrast, the clusters **4** and **5** consist of a butterfly arrangement of the Ru_3Ir framework with the alkyne ligand coordinated to all four metal atoms, giving an overall octahedral Ru_3IrC_2 skeleton, as demonstrated by the single-crystal structure analysis of **4**. Cluster **1** is an excellent catalyst for the hydrogenation of diphenylacetylene to give stilbene (catalytic turnover number 990 within 15 min), clusters **2** and **4** are also catalytically active but seem to represent side-channels of the catalytic cycle.

The synthesis of mixed-metal alkyne clusters has received much attention due to their potential as models for the carbon–carbon triple bond activation on metal surfaces [1,2] and for their catalytic potential in hydrogenation reactions.[3] Different metals in a cluster may also have synergistic effects for catalytic transformations. On the other hand, the increase of the catalytic activity of a transition metal catalyst by addition of another metal complex gives rise to speculations about the formation of mixed-metal clusters to account for the synergistic effect observed.[4]

The reaction of tetranuclear clusters with internal and terminal alkynes often affords the corresponding butterfly complexes where the C_2 unit bonds to the M_4 framework in a $\mu_4\text{-}\eta^2$-fashion to form a quasi-octahedral M_4C_2 skeleton.[5] The co-ordination in a $\mu_3\text{-}\eta^2$-mode of the alkynes on a face of a tetrahedral metal framework is not common and only a few examples have been reported in the literature.[6]

In a recent publication, we have described the synthesis and the reactivity of the mixed-metal cluster $[HIrRu_3(CO)_{13}]$ **1** towards H_2.[7] We now report on the reactivity of **1** towards internal alkynes such as diphenylacetylene and 2–butyne, and on the catalytic activity of **1** in the hydrogenation of diphenylacetylene.

Results and discussion

Synthesis and characterisation of $[HIrRu_3(CO)_{11}(RC{\equiv}CR)]$ (2 R = Ph; 3 R = Me)

The thermal reaction of $[HIrRu_3(CO)_{13}]$ **1** with one equivalent of alkyne in hexane leads to the formation of the new tetrahedral mixed-metal alkyne clusters $[HIrRu_3(CO)_{11}(PhC{\equiv}CPh)]$ **2** and $[HIrRu_3(CO)_{11}(MeC{\equiv}CMe)]$ **3** (Scheme 1). The two complexes **2** and **3**, isolated by chromatographic methods, are stable towards air and moisture. The infrared spectra of clusters **2** and **3** are very similar in the carbonyl region, both presenting six bands in the region of terminal CO vibrations and one absorption at 1842 cm^{-1} (**2**) and 1844 cm^{-1} (**3**) which is attributed to the bridging carbonyl ligand (Table 1).

In the ^1H NMR spectra of **2** and **3**, the hydride signals are observed at higher field with respect to **1**. In the case of **2**, a multiplet centred around δ 7.15 can be assigned to the phenyl protons, whereas in the case of **3** the two methyl groups of the alkyne ligand are equivalent and give only one singlet at δ 2.72, indicating that the alkyne is co-ordinated symmetrically over the Ru_3Ir framework.

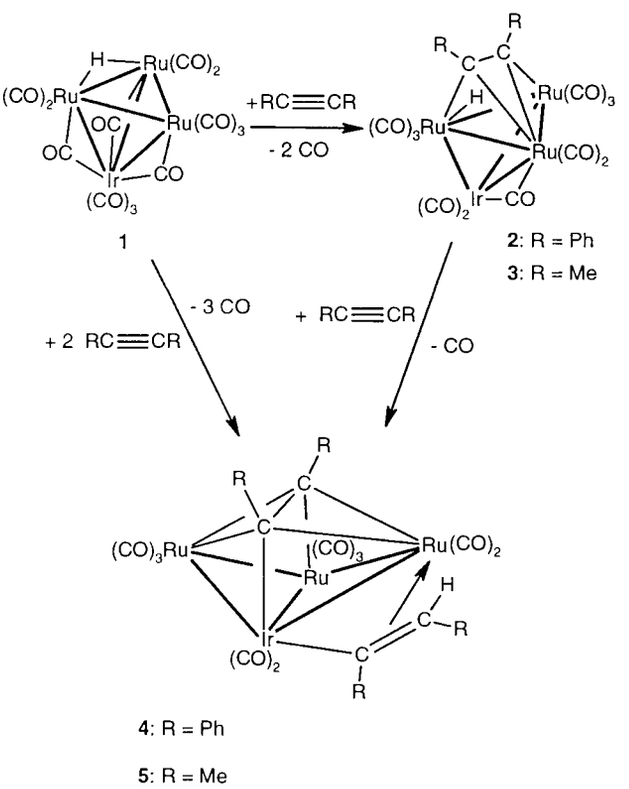

Scheme 1 Synthetic routes to clusters **2**–**5**.

Solid state structures of $[HIrRu_3(CO)_{11}(\mu_3\text{-}\eta^2\text{-}RC{\equiv}CR)]$ (2 R = Ph; 3 R = Me)

The molecular structures of **2** and **3** have been solved by single-crystal X-ray structure analysis. Suitable crystals of **2** and **3**

Table 1 IR and ^{1}H NMR data

Complex	ν(CO)[a]/cm^{-1}	δ[b]
[$HRu_3Ir(CO)_{11}$(PhC≡CPh)] **2**	2095w, 2071s, 2053s, 2037vs, 2012m, 1994m, 1842w	7.30–7.00 (C_6H_5, m), −18.88 (H, s)
[$HRu_3Ir(CO)_{11}$(MeC≡CMe)] **3**	2094w, 2068s, 2049s, 2033vs, 2009m, 1988m, 1844w	2.72 (CH_3, s), −18.98 (H, s)
[$Ru_3Ir(CO)_{10}$(PhC≡CPh)(PhCH=CPh] **4**	2078m, 2043vs, 2037s, 2027m, 2001w, 1990vw, 1964vw	7.70–6.20 (C_6H_5, m), 4.90 (H, s)
[$Ru_3Ir(CO)_{10}$(MeC≡CMe)(MeCH=CMe)][c] **5**	2078m, 2066w, 2043vs, 2032vs, 2014s, 1997m, 1983w, 1959w	4.80 (CH_3CHCCH_3, dq $^3J_{HH}$ 6.1 $^4J_{HH}$ 0.7) 3.09 (CH_3CHCCH_3, d $^4J_{HH}$ 0.7 Hz), 2.90 (CH_3CCCH_3, s) 2.74 (CH_3CCCH_3, s) 1.82 (CH_3CHCCH_3, d $^3J_{HH}$ 6.1 Hz) 4.86 (CH_3CHCCH_3, dq $^3J_{HH}$ 5.95 Hz $^4J_{HH}$ 0.8 Hz) 3.07 (CH_3CHCCH_3), 2.88 (CH_3CCCH_3, s) 2.71 (CH_3CCCH_3, s), 1.77 (CH_3CHCCH_3, d $^3J_{HH}$ 5.95 Hz)

[a] Recorded in dichloromethane **2** and **3**, in hexane **4** and **5**. [b] Measured in $CDCl_3$ solution at 294 K, *J* in Hz. [c] Two isomers in solution (ratio 7:1).

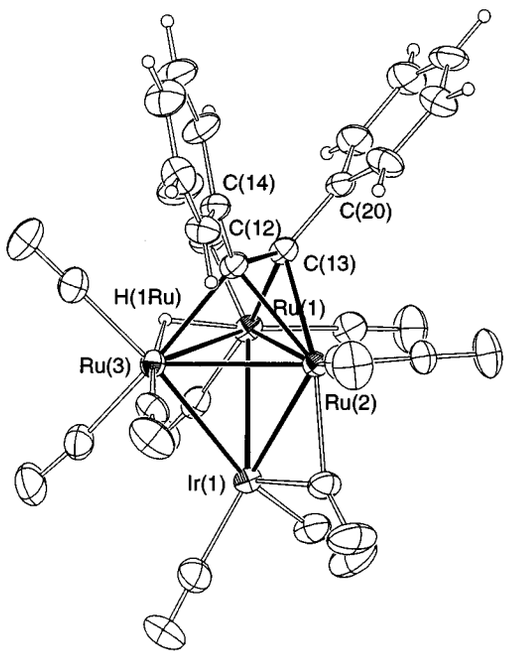

Fig. 1 ORTEP plot of [$HIrRu_3(CO)_{11}(\mu_3$-η^2-$C_2Ph_2)$] **2**. Thermal ellipsoids are drawn at 30% of probability.

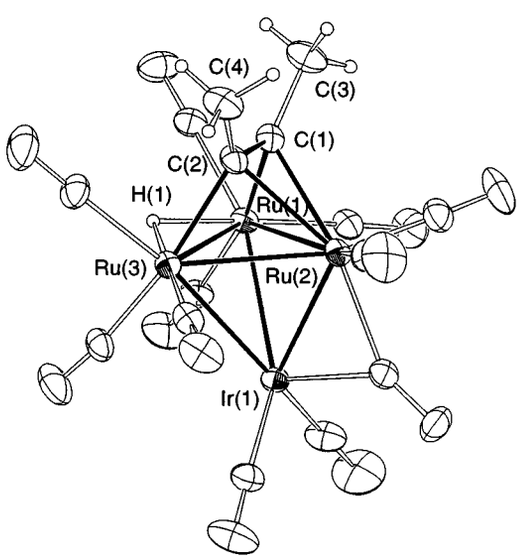

Fig. 2 ORTEP plot of [$HIrRu_3(CO)_{11}(\mu_3$-η^2-$C_2Me_2)$] **3**. Thermal ellipsoids are drawn at 30% of probability.

were grown at −18 °C in hexane. The molecular structure of **2** is depicted in Fig. 1 and that of **3** in Fig. 2. Selected bond lengths and angles of both compounds **2** and **3** are listed in Tables 2 and 3. Both, **2** and **3** have the same overall structure showing the same carbonyl, alkyne and hydride co-ordination. The four metal atoms form a tetrahedron where the Ru–Ir distances vary from 2.6985(7) to 2.8092(7) Å for **2** and from 2.4972(7) to 3.0591(8) Å for **3**. The clusters **2** and **3** present, as expected for a tetrahedral arrangement, an electron count of 60. The short distances Ru(2)–Ir(1) [**2** 2.6985(7); **3** 2.4972(7) Å] are due to the bridging carbonyl ligand over this edge. The base of the tetrahedron is composed of three ruthenium atoms, each of the Ru–Ru distances being different. In both complexes the longer Ru(1)–Ru(3) distance [**2** 2.8513(9); **3** 2.8847(10) Å] suggests the presence of the hydrido bridge across this edge. The hydride ligand in **2** is not symmetrically co-ordinated to the Ru(1)–Ru(3) edge [**2** Ru(1)–HRu(1) 1.51(8), Ru(3)–HRu(1) 1.91(8) Å], whereas in complex **3** the hydride is quasi symmetrically co-ordinated to the Ru(1)–Ru(3) vector [Ru(1)–H(1) 1.76(6)

Table 2 Selected bond lengths (Å) and angles (°) for molecule **2**

Ir(1)–Ru(2)	2.6985(7)	Ru(2)–C(13)	2.208(7)
Ir(1)–Ru(1)	2.7736(8)	Ru(2)–Ru(3)	2.7654(9)
Ir(1)–Ru(3)	2.8092(7)	Ru(3)–C(12)	2.191(8)
Ru(1)–C(13)	2.134(8)	Ru(3)–HRu(1)	1.91(8)
Ru(1)–Ru(2)	2.8476(9)	C(12)–C(13)	1.399(10)
Ru(1)–Ru(3)	2.8513(9)	C(12)–C(14)	1.495(11)
Ru(1)–HRu(1)	1.51(8)	C(13)–C(20)	1.481(11)
Ru(2)–C(12)	2.170(8)		
Ru(2)–Ir(1)–Ru(1)	62.70(2)	Ir(1)–Ru(2)–Ru(1)	59.94(2)
Ru(2)–Ir(1)–Ru(3)	60.24(2)	Ru(3)–Ru(2)–Ru(1)	61.04(2)
Ru(1)–Ir(1)–Ru(3)	61.42(2)	Ru(2)–Ru(3)–Ir(1)	57.90(2)
Ir(1)–Ru(1)–Ru(2)	57.361(19)	Ru(2)–Ru(3)–Ru(1)	60.90(2)
Ir(1)–Ru(1)–Ru(3)	59.91(2)	Ir(1)–Ru(3)–Ru(1)	58.67(2)
Ru(2)–Ru(1)–Ru(3)	58.06(2)	C(13)–C(12)–C(14)	125.8(7)
Ir(1)–Ru(2)–Ru(3)	61.86(2)	C(12)–C(13)–C(20)	124.6(7)

Estimated standard deviations in parentheses.

Table 3 Selected bond lengths (Å) and angles (°) for molecule **3**

Ir(1)–Ru(2)	2.4972(7)	Ru(2)–C(1)	2.446(10)
Ir(1)–Ru(3)	2.7839(7)	Ru(2)–Ru(3)	2.8156(10)
Ir(1)–Ru(1)	3.0591(8)	Ru(3)–C(2)	2.049(8)
Ru(1)–C(1)	1.901(7)	Ru(3)–H(1)	1.75(6)
Ru(1)–Ru(2)	2.8665(10)	C(1)–C(2)	1.385(12)
Ru(1)–Ru(3)	2.8847(10)	C(1)–C(3)	1.534(13)
Ru(1)–H(1)	1.76(6)	C(2)–C(4)	1.388(10)
Ru(2)–C(2)	2.299(9)		
Ru(2)–Ir(1)–Ru(3)	64.17(2)	Ir(1)–Ru(2)–Ru(1)	69.15(2)
Ru(2)–Ir(1)–Ru(1)	61.13(2)	Ru(3)–Ru(2)–Ru(1)	61.01(2)
Ru(3)–Ir(1)–Ru(1)	58.94(2)	Ir(1)–Ru(3)–Ru(2)	52.966(19)
Ru(2)–Ru(1)–Ru(3)	58.62(2)	Ir(1)–Ru(3)–Ru(1)	65.29(2)
Ru(2)–Ru(1)–Ir(1)	49.717(18)	Ru(2)–Ru(3)–Ru(1)	60.37(2)
Ru(3)–Ru(1)–Ir(1)	55.76(2)	C(2)–C(1)–C(3)	129.3(7)
Ir(1)–Ru(2)–Ru(3)	62.87(2)	C(4)–C(2)–C(1)	121.6(8)

Estimated standard deviations in parentheses.

Ru(3)–H(1) 1.75(6) Å]. Two of the three ruthenium atoms are bonded to three terminal CO groups, whereas Ru(2) and Ir(1) are bonded to two terminal CO groups and share the bridging CO ligand. The alkynes are co-ordinated in a μ_3-η^2-bonding mode, which is commonly observed in trinuclear alkyne complexes;[8] compounds **2** and **3** compare well with the mixed-metal clusters $[HCpWOs_3(CO)_{10}(\mu_3\text{-}\eta^2\text{-}C_2Tol_2)]$ (Tol = tolyl)[6a] and with $[H_2Os_4(CO)_9(\mu_3\text{-}\eta^2\text{-}C_2Ph_2)(\eta^2\text{-}C_2Ph_2)]$.[6c] The μ_3-η^2-RCCR ligand (**2** R = Ph; **3** R = Me) lies on the Ru_3 face of the $IrRu_3$ framework and is formally π-bonded to Ru(2) [**2** Ru(2)–C(12) 2.170(8), Ru(2)–C(13) 2.208(7) Å; **3** Ru(2)–C(1) 2.446(10), Ru(2)–C(2) 2.299(9) Å] and is σ-bonded to Ru(1) and Ru(3) [**2** Ru(1)–C(13) 2.134(8), Ru(3)–C(12) 2.191(8) Å; **3** Ru(1)–C(1) 1.901(7), Ru(3)–C(2) 2.049(8) Å]. The formal electron counts at the individual metal atoms are 18.5 for Ru(1) and Ru(3), 18 for Ru(2) and 17 for Ir(1).

The electron deficiency of the Ir atom is apparently compensated for by direct donation from the ruthenium atoms. This is confirmed by the very short Ir(1)–Ru(2) distance [**2** Ir(1)–Ru(2) 2.6985(7); **3** Ir(1)–Ru(2) 2.4972(7) Å] and by the presence of the bridging carbonyl ligand over Ru(2)–Ir(1).

Owing to the co-ordination of the alkyne group to the metal core, the carbon–carbon triple bond is lengthened [**2** C(12)–C(13) 1.399(10); **3** C(1)–C(2) 1.385(12) Å], being in the same range as observed for other clusters such as $[HCpWOs_3(CO)_{10}(\mu_3\text{-}\eta^2\text{-}C_2Tol_2)]$ [isomer 1 1.38(6), isomer 2 1.45(6) Å][6a] and $[H_2Os_4(CO)_9(\mu_3\text{-}\eta^2\text{-}C_2Ph_2)(\eta^2\text{-}C_2Ph_2)]$ [1.44(1) Å].[6c] The alkyne ligands PhC≡CPh and MeC≡CMe are bent, the angles being 125.8(7)° [C(14)–C(12)–C(13)] and 124.6(7)° [C(12)–C(13)–C(20)] for **2**, 129.3(7)° [C(2)–C(1)–C(3)] and 121.6(8)° [C(1)–C(2)–C(4)] for **3**.

A comparison of both structures shows that in **3** the distances Ru(1)–C(1) [1.901(7) Å] and Ru(3)–C(2) [2.049(8) Å] are shorter than the analogous distances in **2** [Ru(1)–C(13) 2.134(8) Å; Ru(3)–C(12) 2.191(8) Å]. These differences in the formal ruthenium–carbon σ-bonds may be explained by steric effects, the methyl substituents being less demanding than the phenyl substituents. For the distances corresponding to the formal ruthenium–carbon π-bonds, the inverse effect is observed. In **3** the distances Ru(2)–C(1) [2.446(10) Å] and Ru(2)–C(2) [2.299(9) Å] are longer than the corresponding distances in **2** [Ru(2)–C(13) 2.208(7) Å; Ru(2)–C(12) 2.170(8) Å], probably due to the higher electron density of 2-butyne with respect to diphenylacetylene.

Synthesis and characterisation of $[IrRu_3(CO)_{10}(RC{\equiv}CR)(RCH{=}CR)]$ (4 R = Ph; 5 R = Me)

Reaction of the tetrahedral alkyne clusters **2** and **3** with a further equivalent of the corresponding alkyne gives the butterfly clusters $[IrRu_3(CO)_{10}(RCCR)(RCH{=}CR)]$ (**4** R = Ph; **5** R = Me), also accessible directly from **1** with at least two equivalents of PhCCPh or MeCCMe (Scheme 1). The infrared spectra of **4** and **5** exhibit almost the same ν(CO) pattern in the area of terminal carbonyls (Table 1). The ^{1}H NMR spectra of **4** and **5** reveal the presence of a vinyl in addition to the alkyne ligand; **4** shows a multiplet centred around δ 6.95 which is assigned to the various phenyl protons. The vinyl proton appears as a singlet at δ 4.90, being characteristic for vinyl complexes.[9] In the case of **5**, the ^{1}H NMR spectrum is more complicated, indicating the presence of two isomers in $CDCl_3$ solution (ratio 7 : 1). We believe the major isomer to be analogous to **4**, whereas in the minor isomer the μ-η^2-$CH_3CH{=}CCH_3$ vinyl ligand is co-ordinated in an inverse fashion with respect to the Ru and Ir atoms. The structure of **4** was confirmed by a single-crystal X-ray structure analysis.

Solid state structure of $[IrRu_3(CO)_{10}(\mu_4\text{-}\eta^2\text{-}PhC{\equiv}CPh)(\mu\text{-}\eta^2\text{-}PhCH{=}CPh)]$ 4

Suitable crystals of **4** were obtained by slow diffusion of methanol into a concentrated dichloromethane solution at room temperature. The molecular structure of **4** is depicted in Fig. 3. Selected bond lengths and angles are presented in Table 4. The cluster **4** is the second compound known with μ_4-η^2-alkyne and a μ-η^2-vinyl ligand co-ordinated to a tetranuclear butterfly skeleton; it compares well with $[FeCo_3(CO)_9(\mu_4\text{-}\eta^2\text{-}PhC{\equiv}CPh)(\mu\text{-}\eta^2\text{-}PhCH{=}CPh)]$.[10] The butterfly backbone consists of a ruthenium and an iridium atom which are bound to two wingtip ruthenium atoms. The Ir(1)–Ru(1) bond distance is longer [2.8311(7) Å] than the other metal–metal distances in **4**, but it is nevertheless in the usual range of the hinge lengths in Ru_4C_2 butterfly complexes.[5,11] The non-bonding Ru(2)···Ru(3) edge [3.9380(5) Å] can be compared to the values of 3.485(4) and 4.123(1) Å reported for the related butterfly clusters $[FeCo_3(CO)_9(\mu_4\text{-}\eta^2\text{-}PhC{\equiv}CPh)(\mu\text{-}\eta^2\text{-}PhCH{=}CPh)]$[10] and $[Co_2Mo_2(\mu_4\text{-}C_2Me_2)(\mu\text{-}CO)_4(CO)_4(\eta^5\text{-}C_5H_5)_2]$,[12] respectively. The dihedral angle between the intersection of the two planes of $IrRu_2$ is 117.27(3)° usual for butterfly clusters.[5b,10] All carbonyl ligands in **4** are terminal (the angles Ir–C–O and Ru–C–O being in the range of 174–179°). Two of the three ruthenium atoms, Ru(1) and Ru(3) are bonded to two CO ligands, whereas Ru(2) and Ir(1) are bonded to three carbonyls.

The PhCCPh ligand interacts with all four metal atoms in a μ_4-η^2-fashion. The carbon–carbon backbone [C(25)–C(26)] is nearly parallel to the Ru(1)–Ir(1) hinge of the cluster, and the torsion angle of the diphenylacetylene unit C(25)–Ir(1)–Ru(1)–C(26) measures 1.9(2)°. The two carbon atoms C(25) and C(26) can be considered as σ-bound to Ir(1) and Ru(1) respectively [Ir(1)–C(25) 2.176(7); Ru(1)–C(26) 2.194(7) Å] and as π-bound

Table 4 Selected bond lengths (Å) and angles (°) for molecule **4**

Ir(1)–C(11)	2.115(6)	Ru(2)–C(25)	2.250(6)
Ir(1)–C(25)	2.176(7)	Ru(2)–C(26)	2.283(6)
Ir(1)–Ru(3)	2.6518(6)	Ru(3)–C(11)	2.185(6)
Ru(2)···Ru(3)	3.9380(5)	Ru(3)–C(26)	2.250(6)
Ir(1)–Ru(2)	2.7373(7)	Ru(3)–C(12)	2.262(7)
Ir(1)–Ru(1)	2.8311(7)	Ru(3)–C(25)	2.290(7)
Ru(1)–C(26)	2.194(7)	C(11)–C(12)	1.419(10)
Ru(1)–Ru(3)	2.7101(8)	C(12)–H(12)	1.03(8)
Ru(1)–Ru(2)	2.7233(9)	C(25)–C(26)	1.431(10)
C(12)–C(11)–C(13)	122.6(5)	C(26)–C(25)–C(27)	127.9(6)
C(11)–C(12)–C(19)	127.5(6)	C(25)–C(26)–C(33)	125.5(7)
Ru(3)–Ir(1)–Ru(1)–Ru(2)	117.27(3)		

Estimated standard deviations in parentheses.

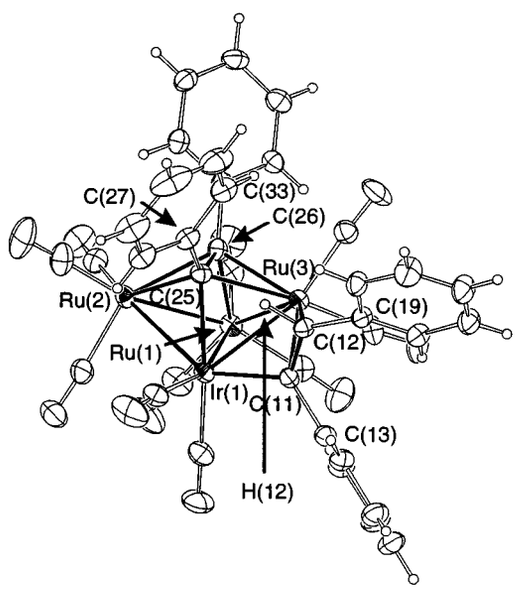

Fig. 3 ORTEP plot of $[IrRu_3(CO)_{10}(\mu_4\text{-}\eta^2\text{-}C_2Ph_2)(\mu\text{-}\eta^2\text{-}PhCH{=}CPh)]$ **4**. Thermal ellipsoids are drawn at 30% of probability.

Table 5 Catalytic hydrogenation of diphenylacetylene

Catalyst	Product (%)				TON	TOF/min^{-1}
	PhCCPh	*trans*-PhCHCHPh	*cis*-PhCHCHPh	$PhCH_2CH_2Ph$		
$[HIrRu_3(CO)_{13}]$	0	98.8	0.2	1	990	66
$[H_3IrRu_3(CO)_{12}]$	17	48.5	33	1.5	815	54
$[HIrRu_3(CO)_{11}(PhCCPh)]$	6	73	18	3	910	60
$[HIrRu_3(CO)_{10}(PhCCPh)(PhCH{=}CPh)]$	30	30	37	3	670	45

Conditions: $P(H_2) = 10$ bar, $T = 120$ °C, hexane = 30 ml, $t = 15$ min. Catalyst: 1.174×10^{-5} mol. Catalyst–substrate ratio 1:1000. TOF: catalytic turnover frequency, TON: catalytic turnover number.

Table 6 Catalytic hydrogenation of diphenylacetylene in presence of CO

Catalyst	Product (%)				TOF/min^{-1}	*t*/min
	PhCCPh	*trans*-PhCHCHPh	*cis*-PhCHCHPh	$PhCH_2CH_2Ph$		
$[HIrRu_3(CO)_{13}]$	0.1	4.4	95.3	0.09	16	30
$[H_3IrRu_3(CO)_{12}]$	2	3	95	0	11	45
$[HIrRu_3(CO)_{11}(PhCCPh)]$	0.5	4.4	95	0.08	13	40
$[HIrRu_3(CO)_{10}(PhCCPh)(PhCH{=}CPh)]$	0	16	80	0	11	45

Conditions: $P(H_2) = 9$ bar, $P(CO) = 1$ bar, $T = 120$ °C, hexane = 30 ml. Catalyst: 1.174×10^{-5} mol. Catalyst–substrate ratio 1:500. TOF: catalytic turnover frequency.

to the two wingtip ruthenium atoms [Ru(2)–C(25) 2.250(6); Ru(2)–C(26) 2.283(6); Ru(3)–C(26) 2.250(6); Ru(3)–C(25) 2.290(7) Å].

Owing to the co-ordination to the four metal atoms, the C–C bond is longer [C(25)–C(26) 1.431(10) Å] than in clusters **2** and **3**. The vinyl ligand is co-ordinated to Ir(1) and Ru(3) in a classical μ-η^2-mode; the C(11)–C(12) group is σ-bound to Ir(1) [Ir(1)–C(11) 2.115(6) Å] and is π-bound to Ru(3) [Ru(3)–C(11) 2.185(6); Ru(3)–C(12) 2.262(7) Å]. Also due to the co-ordination to the metal framework the C–C bond is lengthened [C(25)–C(26) 1.431(10) Å] with respect to a free carbon–carbon double bond.

With an electron count of 60, cluster **4** is electron-deficient, since a M_4 butterfly cluster consistent with the noble gas rule would require 62 electrons. However, considering **4** as an octahedral Ru_3IrC_2 cluster, it is consistent with Wade's rules predicting a *closo*-structure.[13]

Catalytic hydrogenation of diphenylacetylene

The mixed-metal cluster $[HIrRu_3(CO)_{13}]$ **1** turned out to be an excellent catalyst for the hydrogenation of diphenylacetylene in hexane solution (Table 5). Within 15 min, the substrate is completely converted, the catalyst–substrate ratio being 1:1000, the catalytic turnover frequency (TOF) being 66 min^{-1} (120 °C, 10 bar). The selectivity is very high, giving 98.8% *trans*-stilbene, 0.2% *cis*-stilbene and 1% 1,2-diphenylethane. The main product, *trans*-stilbene precipitates directly from the reaction mixture.

At the end of the catalytic reaction, the yellow solution contains the intact $IrRu_3$ cluster system however, it is not the $[HIrRu_3(CO)_{13}]$ complex employed but $[H_3IrRu_3(CO)_{12}]$ which forms quantitatively from $[HIrRu_3(CO)_{13}]$ under hydrogen pressure.[7] $[H_3IrRu_3(CO)_{12}]$ as well as the alkyne derivatives isolated, $[IrRu_3(CO)_{10}(\mu_3\text{-}\eta^2\text{-}PhC{\equiv}CPh)]$ **2** and $[IrRu_3(CO)_{10}(\mu_4\text{-}\eta^2\text{-}PhC{\equiv}CPh)(\mu\text{-}\eta^2\text{-}PhCH{=}CPh)]$ **4**, also catalyse the hydrogenation of diphenylacetylene. However, the selectivities and activities are not as good as in the case of $[HIrRu_3(CO)_{13}]$ **1** (Table 5). If the hydrogenation is carried out in the presence of carbon monoxide (H_2–CO 9:1), both selectivity and activity decrease (Table 6). In particular, it is interesting to note that under these conditions the main product is *cis*-stilbene.

On the basis of these findings, the recovery of the intact $IrRu_3$ cluster, and the isolation and characterisation of the two acetylene derivatives $[IrRu_3(CO)_{11}(\mu_3\text{-}\eta^2\text{-}PhC{\equiv}CPh)]$ **2** and $[IrRu_3(CO)_{10}(\mu_4\text{-}\eta^2\text{-}PhC{\equiv}CPh)(\mu\text{-}\eta^2\text{-}PhCH{=}CPh)]$ **4**, we propose a tentative mechanism involving intact $IrRu_3$ intermediates for the catalytic hydrogenation of diphenylacetylene (Scheme 2). The cluster $[HIrRu_3(CO)_{13}]$ **1** can react with the alkyne under CO substitution to give an intermediate $[HIrRu_3(CO)_{12}(PhC{\equiv}CPh)]$. After hydrogen transfer from the metal framework onto the co-ordinated alkyne, the vinyl species $[IrRu_3(CO)_{12}(PhCH{=}CPh)]$ is formed. Uptake of molecular hydrogen should give $[H_2IrRu_3(CO)_{12}(PhCH{=}CPh)]$ which, after reaction with CO gives stilbene and the catalyst $[HIrRu_3(CO)_{13}]$ **1** (cycle A). Under the reaction conditions (H_2 pressure) the catalyst is converted into $[H_3IrRu_3(CO)_{12}]$, the only organometallic species detected (by IR spectroscopy) at the end of the reaction and which can be isolated. This cycle parallels the hydrogenation mechanism proposed by Cabeza *et al.* using the trinuclear cluster $[HRu_3(CO)_9(ampy)]$ (Hampy = 2-amino-6-methylpyridine) as the catalyst.[14] We consider the two alkyne clusters **2** and **4** which we isolated from the reaction of **1** with diphenylacetylene to be members of a side channel which operates only in the absence of hydrogen. The hydrogenated species $[H_3IrRu_3(CO)_{12}]$ also reacts with the alkyne to give, with formation of the corresponding olefin, the intermediate $[HIrRu_3(CO)_{12}(PhC{\equiv}CPh)]$ (cycle B). This is in accordance with the observation that **1** reacts more rapidly with H_2 than with diphenylacetylene. The infrared spectrum shows that under a pressure of 2 bar of H_2 at 120 °C (after 2 min), **1** is quantitatively converted into $[H_3IrRu_3(CO)_{12}]$, in the presence or absence of diphenylacetylene.

Experimental

All reactions were carried out in an atmosphere of pure nitrogen using standard Schlenk techniques. Solvents were distilled over appropriate drying agents and deoxygenated and nitrogen-saturated prior to use.[15] Preparative thin-layer chromatography was performed using 20 × 20 cm plates coated with Fluka silica gel G. The starting complex $[HIrRu_3(CO)_{13}]$ was prepared according to the published method.[7] Diphenylacetylene and octadecane were purchased from Fluka, *cis*- and *trans*-stilbene as well as 1,2-diphenylethane were purchased from Aldrich and used as received. NMR spectra were recorded using a Varian Gemini 200 BB or a Bruker AMX 400 spectrometer, using the resonance of the residual protons of the deuteriated solvents as reference. Infrared spectra were recorded with a Perkin-Elmer 1720X FT-IR spectrometer. Mass spectra were measured by

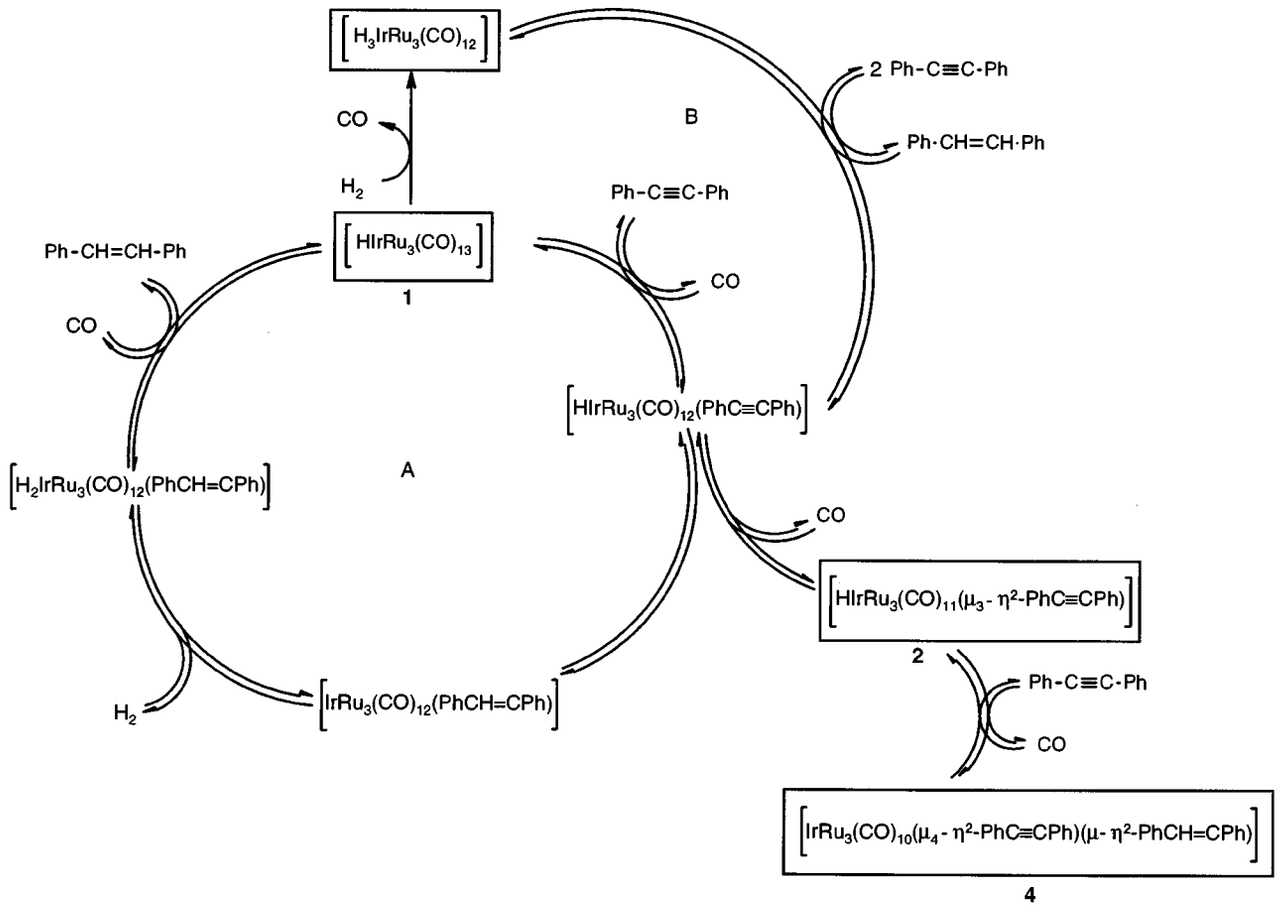

Scheme 2 Proposed mechanism for the catalytic hydrogenation of diphenylacetylene catalysed by $[HIrRu_3(CO)_{13}]$. Isolated and fully characterised species are indicated by a frame.

Professor T. A. Jenny at the University of Fribourg, Switzerland. Microanalyses were carried out by the Mikroelementaranalytisches Laboratorium of the ETH Zürich, Switzerland. GC spectra were recorded with a DANI 86.10 gas chromatograph using a Chrompack (WCOT fused silica 25 M X 0.32 mm) capillary column and octadecane as internal standard.

Preparations

$[HIrRu_3(CO)_{11}(PhC{\equiv}CPh)]$ 2. A solution of $[HIrRu_3(CO)_{13}]$ **1** (73 mg, 0.085 mmol) and PhC≡CPh (15 mg, 0.085 mmol) in hexane (30 ml) was stirred at 80 °C in a pressure Schlenk tube. During the reaction the pressure was released once. After 1 h the solution changed from red to orange. After removal of the solvent, the dark orange residue was dissolved in 5 ml of CH_2Cl_2 and submitted to thin-layer chromatography (silica gel, CH_2Cl_2–hexane 1 : 3). Two main bands were obtained. The first one contained $[IrRu_3(CO)_{10}(PhC{\equiv}CPh)(PhCH{=}CPh)]$ **4** (9.1 mg, 11%). The second one (orange) contained **2**, it was extracted with CH_2Cl_2 and recrystallised from hexane at −18 °C. The FAB mass spectrum of **2** shows the molecular peak at *m/z* 985 (^{102}Ru, ^{191}Ir), followed by a fragmentation series of $[HIrRu_3(CO)_n(PhC{\equiv}CPh)]$ (n = 1–10). The orange air-stable crystals were dried *in vacuo.* Yield 17.3 mg, 23% (Found: C, 30.64; H, 1.11. $C_{25}H_{11}O_{11}Ru_3Ir$ requires C, 30.55; H, 1.13%).

$[HIrRu_3(CO)_{11}(CH_3C{\equiv}CCH_3)]$ 3. A solution of $[HIrRu_3(CO)_{13}]$ **1** (100 mg, 11.6 mmol) and a slight excess of cold $CH_3C{\equiv}CCH_3$ (10 μl, 12.8 mmol) in hexane (30 ml) was stirred at 85 °C in a pressure Schlenk tube. During the reaction the pressure was released once. After 90 min the solution had changed from red to orange. After removal of the solvent, the dark orange residue was dissolved in 5 ml of CH_2Cl_2 and purified by thin layer chromatography (silica gel, CH_2Cl_2–hexane 1 : 3). Two bands were obtained, the first one contained $[IrRu_3(CO)_{10}(CH_3C{\equiv}CCH_3)(CH_3CH{=}CCH_3)]$ **5** (3 mg, 3%), the second one (orange) contained **3**. The product was extracted with CH_2Cl_2 and recrystallized from hexane at −18 °C. The orange air-stable crystals were dried *in vacuo.* Yield 40 mg, 40% (Found: C, 21.01; H, 0.78. $C_{15}H_7O_{11}Ru_3Ir$ requires C, 20.98; H, 0.82%).

$[IrRu_3(CO)_{10}(PhC{=}CPh)(PhCH{=}CPh)]$ 4. A solution of $[HIrRu_3(CO)_{13}]$ **1** (100 mg, 11.6 mmol) and PhC≡CPh (62 mg, 34.8 mmol) in hexane (30 ml) was stirred at 85 °C in a pressure Schlenk tube. During the reaction the pressure was released once. After 90 min the solution had changed from red to dark brown. After removal of the solvent, the dark brown residue was dissolved in 5 ml of CH_2Cl_2 and purified by thin layer chromatography (silica gel, CH_2Cl_2–hexane 1 : 3). Cluster **4** was extracted from the main brown band with CH_2Cl_2 and recrystallized at room temperature from a biphasic mixture of CH_2Cl_2–MeOH. The black air-stable crystals were dried *in vacuo*. Yield 53 mg, 40% (Found: C, 40.56; H, 1.74. $C_{38}H_{21}O_{10}Ru_3Ir$ requires C, 40.28; H, 1.87%). The product **4** is also accessible from **2** (17.3 mg, 0.0176 mmol) and PhC≡CPh (3.45 mg 0.0176 mmol) by heating in hexane (30 ml, 90 °C, 60 min, one pressure release) in 78% yield after thin-layer chromatography.

$[IrRu_3(CO)_{10}(CH_3C{\equiv}CCH_3)(CH_3CH{=}CCH_3)]$ 5. A solution of $[HIrRu_3(CO)_{13}]$ **1** (100 mg,11. 62 mmol) and a large excess of $CH_3C{\equiv}CCH_3$ (91 μl, 116. 2 mmol) in hexane (30 ml) was stirred at 85 °C in a pressure Schlenk tube. During the reaction the pressure was released once. After 4 hours the solution had changed from red to dark yellow. After removal of the solvent,

Table 7 Crystallographic graphic data and refinement details for compounds **2**, **3** and **4**

	2	**3**	**4**
Formula	$C_{25}H_{11}IrO_{11}Ru_3$	$C_{15}H_7IrO_{11}Ru_3$	$C_{38}H_{21}IrO_{10}Ru_3$
M	982.75	858.62	1132.96
Crystal system	Monoclinic	Monoclinic	Triclinic
Space group	$P2_1/n$	$P2/c$	$P\bar{1}$
a/Å	9.3321(14)	14.0189(12)	9.7805(9)
b/Å	32.744(3)	9.6264(15)	10.9610(10)
c/Å	9.3486(15)	15.7007(6)	18.1569(16)
α/°	90	90	83.294(11)
β/°	98.413(12)	90.005(5)	85.845(11)
γ/°	90	90	69.536(10)
U/Å^3	2825.9(7)	2118.8(4)	1810.1(3)
Z	4	4	2
Crystal size/mm	0.38 × 0.38 × 0.27	0.34 × 0.34 × 0.23	0.30 × 0.23 × 0.15
Colour	Red	Orange	Black
D_c/g cm^{-3}	2.310	2.692	2.079
μ/mm^{-1}	6.323	8.411	4.949
Transmission factors: min/max	0.0595/0.1764	0.0404/0.1376	0.170/0.642
F(000)	1832	1576	1076
θ limits/°	2.29–25.49	2.12–28.79	2.22–25.88
hkl ranges	−11 to 11, 0 to 39, 0 to 11	−19 to 0, 0 to 11, −16 to 16	−11 to 11, −13 to 13, −22 to 21
Reflections measured	5254	3956	14184
Independent reflections	5254	3956	6501
Observed reflections	4596	3479	5168
$R1[I > 2\sigma(I)]/R1$ (all data)[a]	0.0366/0.0478	0.0359/0.0443	0.0349/0.0469
$wR2[I > 2\sigma(I)]/wR2$ (all data)[b]	0.0735/0.0820	0.0824/0.0876	0.0890/0.0922
Goodness of fit on F^2[c]	1.130	1.129	1.024
Maximum δ/σ	0.000	0.001	0.001
Largest difference peak and hole/e Å^3	0.932/−0.912	1.406/−1.162	1.187/−0.943

[a] $R1 = \Sigma||F_o| - |F_c||/\Sigma|F_o|$. [b] $wR2 = [\Sigma w(F_o^2 - F_c^2)^2/\Sigma w(F_o)^4]^{\frac{1}{2}}$. [c] $S = [\Sigma w(F_o^2 - F_c^2)^2/(n - p)]^{\frac{1}{2}}$ (n = number of reflections, p = number of parameters).

the dark brown residue was dissolved in 5 ml of CH_2Cl_2 and purified by thin layer chromatography (silica gel, CH_2Cl_2–hexane 1:4). Complex **5** (existing as a mixture of two isomers) was extracted from the main brown band with CH_2Cl_2 and was precipitated as a brown powder from methanol–pentane at 28 °C. The powder was dried *in vacuo*. Yield 13.2 mg, 13% (Found: C, 25.23; H, 2.38. $C_{18}H_{13}O_{10}Ru_3Ir{\cdot}2CH_3OH$ requires C, 25.32; H, 2.23%). The product **5** is also accessible from **3** (57 mg, 66.4 mmol) and an excess of $CH_3C{\equiv}CCH_3$ (50 μl, 10 equivalents) by heating in hexane (30 ml, 90 °C, 3 hours, one pressure release) in 41% yield after thin-layer chromatography.

Catalytic runs

In a typical experiment, 1.174×10^{-5} mol of the catalyst were dissolved in hexane (30 ml). To this solution, placed in a 100 ml stainless-steel autoclave, 1000 equivalents of the substrate were added. After purging three times with H_2, the autoclave was pressurised with hydrogen (10 bar) and heated to 120 °C under vigorous stirring of the reaction mixture. After the reaction time indicated in Tables 5 and 6, the autoclave was cooled to room temperature and the pressure released. The reaction mixture was then analysed by gas chromatography.

Crystallography

Single crystals of **2** and **3** were obtained in hexane at −18 °C, whereas **4** was recrystallized at room temperature by diffusion of methanol into CH_2Cl_2. Selected crystallographic data for the three complexes are summarised in Table 7 and significant bond lengths and bond angles are listed in Tables 2, 3 and 4.

Data collection, solution and structure refinement. Single-crystal X-ray diffraction data of **2** and **3** were collected at room temperature on a Stoe-Siemens AED2-four circle diffractometer using Mo-Kα graphite-monochromated radiation (λ = 0.71073 Å; ω–2θ scans) and for **4** on a Stoe Imaging Plate Diffractometer System (Stoe & Cie, 1995) equipped with a one-circle goniometer and a graphite-monochromator. 200 exposures (3 min per exposure) were obtained at an image plate distance of 70 mm with $0 < \varphi < 200°$ and with the crystal oscillating through 1° in φ. The resolution was $D_{min} - D_{max}$ 0.81–12.45 Å. The structures were solved by direct methods using the program SHELXS-97[16] and refined by full matrix least squares on F^2 with SHELXL-97.[17] The positions of the hydrides in **2** and **3** as well as the vinyl proton in **4** were located from Fourier-difference maps and refined isotropically, while the remaining hydrogen atoms were included in calculated positions and treated as riding atoms using SHELXL-97 default parameters. For **2** and **3** an empirical absorption was applied based on ψ scans[18] and for **4** using DIFABS.[19] Crystallographic details are given in Table 7 and significant bond lengths and bond angles are listed in Tables 2, 3 and 4. The Figures were drawn with ORTEP[20] (thermal ellipsoides, 30% probability level).

CCDC reference number 186/1194.

See http://www.rsc.org/suppdata/dt/1998/3825/ for crystallographic files in .cif format.

Acknowledgements

We thank the Fonds National Suisse de la Recherche Scientifique for financial support of this work. A generous loan of ruthenium(III) chloride hydrate from the Johnson Matthey Research Centre is gratefully acknowledged.

References

1 E. Sappa, A. Tiripicchio and P. Braunstein, *Chem. Rev.*, 1983, **83**, 203.
2 N. T. Allison, J. R. Fritch, K. P. C. Vollhardt and E. C. Walborsky, *J. Am. Chem. Soc.*, 1983, **105**, 1384; A. D. Clauss, J. R. Shapley, C. N. Wilkes and R. Hoffmann, *Organometallics*, 1984, **3**, 169; J. R. Fox, W. L. Gladfelter, G. L. Goeffroy, I. Tavanaiepour, S. Abdel-Mequid and V. W. Day, *Inorg. Chem.*, 1981, **20**, 3230; E. Roland and H. Vahrenkamp, *Organometallics*, 1983, **2**, 183.
3 G. Süss-Fink and M. Jahncke, *Synthesis of Organic Compounds Catalysed by Transition Metal Clusters*, in *Catalysis by Di- and Polynuclear Metal Cluster Complexes*, ed. R. D. Adams and F. A. Cotton, Wiley-VCH, Chichester, 1998, ch. 6, p. 167.

4 G. Süss-Fink and F. Neumann, *The Use of Transition Metal Clusters in Organic Synthesis*, in *The Chemistry of the Metal-Carbon Bond*, ed. F. R. Hartley, Wiley, Chichester, 1989, vol. 5, ch. 7, p. 231.
5 (*a*) R. K. Pomeroy, *Tetranuclear Clusters of Ruthenium and Osmium*, in *Comprehensive Organometallic Chemistry 2*, ed. E. W. Abel, F. G. A. Stone and G. Wilkinson, Elsevier, Oxford, 1995, vol. 7, ch. 15, p. 835; (*b*) E. Sappa, A. Tiripicchio, A. J. Carty and G. E. Toogood, *Prog. Inorg. Chem.*, 1987, **35**, 437.
6 (*a*) J. T. Park, J. R. Shapley, C. Bueno, J. W. Ziller and M. Rowen Churchill, *Organometallics*, 1988, **7**, 2307; (*b*) J. T. Park, J. R. Shapley, M. Rowen Churchill and C. Bueno, *J. Am. Chem. Soc.*, 1983, **105**, 6182; (*c*) H. Chen, B. F. G. Johnson, J. Lewis, D. Braga, F. Grepioni and P. Sabatino, *J. Organomet. Chem.*, 1991, **405**, C22; (*d*) U. Riaz, M. D. Curtis, A. Rheingold and B. S. Haggerty, *Organometallics*, 1990, **9**, 2647; (*e*) Ming-Tsun Kuo, Der-Kweng Hwang, Chao-Shiuan Liu, Yun Chi, Shie-Ming Peng and Gene-Hsiang Lee, *Organometallics*, 1994, **13**, 2142.
7 G. Süss-Fink, S. Haak, V. Ferrand and H. Stoeckli-Evans, *J. Chem. Soc.*, *Dalton Trans.*, 1997, 3861.
8 S. Deabate, R. Giordano, E. Sappa, *J. Cluster Sci.*, 1997, **8**, 407.
9 V. Ferrand, K. Merzweiler, G. Rheinwald, G. Süss-Fink and H. Stoeckli-Evans, *J. Organomet. Chem.*, 1997, **549**, 263 and refs. therein.
10 S. Aime, D. Osella, L. Milone, A. M. Manotti Lanfredi and A. Tiripicchio, *Inorg. Chim. Acta*, 1983, **71**, 141.
11 P. Mathur, S. Ghosh, Md. Munkir Hossain, C. V. V. Satyanarayana, A. L. Rheingold and G. P. A. Yap, *J. Organomet. Chem.*, 1997, **538**, 57 and refs. therein; A. A. Koridze, A. M. Sheloumov, F. M. Dolgushin, A. I. Yanovsky, Y. T. Struchkov and P. V. Petrovskii, *J. Organomet. Chem.*, 1997, **536**, 381.
12 H. Adams, N. A. Barley, L. J. Gill, M. J. Morris and T. A. Wildgoose, *J. Chem. Soc.*, *Dalton Trans.*, 1996, 1437.
13 K. Wade, *Adv. Inorg. Chem. Radiochem.*, 1976, **18**, 1.
14 J. A. Cabeza, J. M. Ferandez-Colinas and A. Llamazares, *Synlett*, 1995, 579.
15 D. D. Perrin and W. L. F. Armarego, *Purification of Laboratory Chemicals*, Pergamon Press, Oxford, 3rd edn., 1988.
16 G. M. Sheldrick, *Acta Crystallogr.*, *Sect. A*, 1990, **46**, 467.
17 G. M. Sheldrick, SHELXL-97, Program for crystal structure refinement, University of Göttingen, 1997.
18 A. C. T. North, D. C. Phillips and F. C. Mathews, *Acta Crystallogr.*, *Sect. A*, 1968, **24**, 351.
19 N. Walker and D. Stuart, *Acta Crystallogr.*, *Sect. A*, 1990, **46**, 158.
20 C. K. Johnson, ORTEP, Oak Ridge National Laboratory, Oak Ridge, TN, modified for PC by L. Zsolnai and H. Pritzkow, University of Heidelberg, Germany, 1994.

Paper 8/05852K